European Journal of Chemistry

Journal webpage: www.eurjchem.com

Synthesis, structural and spectral characterization, and in vitro nuclease activity of new thiosemicarbazone derivatives

Mouayed Abdulaali Hussein [1,2,*] and Teoh Siang Guan [2]

[1] *Department of Chemistry, College of Science, University of Basrah, Basrah, 61001, Iraq*
[2] *School of Chemical Science, Universiti Sains Malaysia, Minden, Pulau Pinang, 11800, Malaysia*

** Corresponding author at: Department of Chemistry, College of Science, University of Basrah, Basrah, 61001, Iraq.*
Tel.: +964.40.7800196370. Fax: +964.40.7800196370. E-mail address: mouayed_505emar@yahoo.com (M. Hussein).

ARTICLE INFORMATION

DOI: 10.5155/eurjchem.7.1.1-7.1354

Received: 01 November 2015
Received in revised form: 16 November 2015
Accepted: 18 November 2015
Published online: 31 March 2016
Printed: 31 March 2016

KEYWORDS

DNA cleavage
Gel electrophoresis
Thiosemicarbazone
Electronic transition
Fluorescence emission
X-ray single crystal structure

ABSTRACT

Two new compounds, (*E*)-2-(3-ethoxy-2-hydroxybenzylidene)hydrazinecarbothioamide (1) and (*E*)-*N*-ethyl-2-((2-hydroxynaphthalen-1-yl)methylene)hydrazinecarbothioamide (2) have been synthesized. The prepared compounds have been characterized by CHN analysis, FT-IR, UV-Vis, ^{1}H and ^{13}C NMR spectroscopic techniques as well as the fluorescence emission spectroscopy. The molecular structures of the compounds have also been determined by X-ray single crystal diffraction analysis. The crystal structures revealed that the compounds are remain as a thione form in the solid state and are different in their geometrical, conformational and symmetrical structures. The nuclease activity of compounds to cleave pBR 322 has been investigated using agarose gel electrophoresis assay. The compound 2 revealed a significant nuclease activity which was attributed to the lipophilic properties that provided by substituent moieties of the compound.

Cite this: *Eur. J. Chem.* **2016**, *7(1)*, 1-7

1. Introduction

Thiosemicarbazones have received more attention due to their chemotherapeutic applications [1-4]. Thiosemicarbazones are important compounds because of their antiviral, antimalarial, antifungal and antitumor activities [5-9]. The biological activity of thiosemicarbazones are a function for their aldehyde or ketone moiety, which acts as a tridentate ONS donor ligands and provide a suitable complexation structure for many transition metals [10-14]. Thiosemicarbazones ligands attract considerable attention because they are straightforward to synthesize and have scope for structural diversity [15,16]. Recent studies showed the biological activities of thiosemicarbazones especially the antitumor activity are a function of their geometrical and conformational structures, the most active thiosecarbazones are that possess the *trans* isomer [17-20]. The ability of compounds to cleave DNA has received more attention because of such compounds can be used as agents in biotechnology, structural studies of nucleic acids, or development of new drugs [21-23]. Thiosecarbazones are one of a suitable chelating agents for metal ions which can be using as artificial nucleases because of their various structural features and their ability to change their redox potential during coordinated with these ligands [24,25].

To our best knowledge, there is still very little information available regarding the DNA cleavage by thiosemicarbazones. Here, we present the synthesis, spectral characterization, X-ray single crystal structure and nuclease activity to cleave pBR 322 plasmid DNA for two new thiosemicarbazone compounds.

2. Experimental

2.1. Materials and methods

All the reagents and solvents were purchased from Sigma-Aldrich were of reagent grade and used without further purification. Melting point was measured by the Stuart Scientific SMP1 melting point apparatus. FT-IR spectra were recorded on a Perkin Elmer System 2000 spectrophotometer using the KBr disc method. UV-Visible spectra were recorded on a Perkin Elmer Lambda-35 spectrophotometer. Fluorescence spectra were recorded on a Jasco FP-750 spectrophotometer. ^{1}H NMR and ^{13}C NMR spectra were recorded on a Bruker 500 MHz using DMSO-d_6 as the solvent. The chemical shift values are reported in ppm from TMS.

ISSN 2153-2249 (Print) / ISSN 2153-2257 (Online)
http://dx.doi.org/10.5155/eurjchem.7.1.1-7.1354

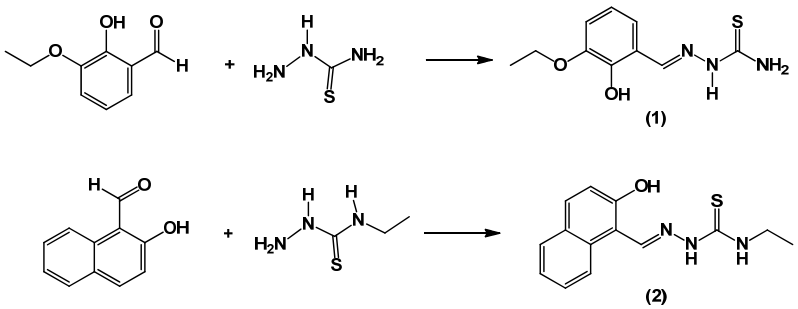

Scheme 1

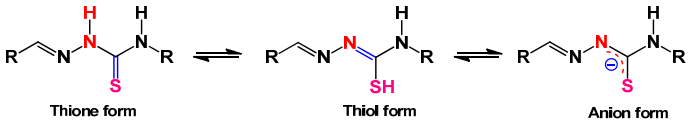

Scheme 2

Elemental analysis was conducted using a Perkin Elmer 2400 Series-11 CHN analyzer. X-ray crystallographic data were recorded on a Bruker SMART APEXII CCD area-detector diffractometer using graphite monochromated MoKα radiation (λ = 0.71073 Å) at 100 K. The data were collected and reduced using APEX2 and SAINT programs. The structure of all compounds was solved using the SHELXS-97 program package, and refined using the SHELXL-97 program package. All non-hydrogen atoms were anisotropically refined. The molecular graphics were created using SHELXTL-97 [26].

2.2. Nuclease activity assay

The nuclease activity of compound **1** and **2** to cleave pBR322 plasmid DNA was studied using agarose gel electrophoresis technique in Tris/EDTA buffer solution. The samples were prepared by mixing appropriate quantities from DNA, compound and H_2O_2. Then incubated at 37 °C for 2 h, treated with loading dye, and electrophoresed for 1 h at 50 V on 1% agarose gel consisting of 12 lanes: lane 1, pBR322 DNA (0.025 μM); lane 2, DNA (0.025 μM) + compound (6 μM); lane 3, DNA (0.025 μM) + H_2O_2 (4.5 μM); lane 4, DNA (0.025 μM) + H_2O_2 (4.5 μM) + compound (1 μM); lane 5, DNA (0.025 μM) + H_2O_2 (4.5 μM) + compound (2 μM); lane 6, DNA (0.025 μM) + H_2O_2 (4.5 μM) + compound (3 μM); lane 7, DNA (0.025 μM) + H_2O_2 (4.5 μM) + compound (3.5 μM); lane 8, DNA (0.025 μM) + H_2O_2 (4.5 μM) + compound (4 μM); lane 9, DNA (0.025 μM) + H_2O_2 (4.5 μM) + compound (4.5 μM); lane 10, DNA (0.025 μM) + H_2O_2 (4.5 μM) + compound (5 μM) and lane 11, DNA (0.025 μM) + H_2O_2 (4.5 μM) + compound (6 μM). The gel was then stained with ethidium bromide before being photographed under UV light. The results were controlled using 1 kbp ladder DNA (lane, L).

2.3. General procedure for the synthesis of compound 1 and 2

A solution of the corresponding aldehyde in ethanol (20 mL) was added to an ethanolic solution (20 mL) of thiosemicarbazide (5.48 mmol) or 4-ethyl-3-thiosemicarbazide (4.19 mmol). The resulting yellow solution was refluxed with stirring for 2 h (Scheme 1). The product was isolated by filtration, washed with ethanol and dried. Plate colorless and needle yellow were obtained by slow evaporation of DMF for compound **1** and **2**, respectively.

(*E*)-2-(3-Ethoxy-2-hydroxybenzylidene)hydrazinecarbothioamide (**1**): Yield: 79%. M.p.: 181-183 °C. FT-IR (KBr, ν, cm^{-1}): 3317 (OH), 1609 (C=N), 1550 ($C_{aro}O$), 1275 (C=S). ^1H NMR (500 MHz, DMSO-d_6, δ, ppm): 1.37 (t, 3H, CH_3), 4.04 (q, 2H, CH_2), 6.57 (t, 1H, Ar-H), 6.91 (d, 1H, Ar-H), 7.50 (d, 1H, Ar-H), 7.87 (s, 1H, NH_2), 8.03 (s, 1H, NH_2), 8.41 (s, 1H, CH=N), 9.13 (br, 1H, OH), 11.40 (s, 1H, N-NH). ^{13}C NMR (125 MHz, DMSO-d_6, δ, ppm): 14.50 (CH_3), 64.15 (CH_2), 114.06-146.17 (C-Aromatic), 146.95 (C=N), 177.51 (C=S), Anal. calcd. for $C_{10}H_{13}N_3O_2S$: C, 50.19; H, 5.48; N, 17.56. Found: C, 50.17; H, 5.48; N, 17.52%. UV-Vis (DMSO, λ_{max}, nm): 295, 312.

(*E*)-*N*-Ethyl-2-((2-hydroxynaphthalen-1-yl) methylene) hydrazinecarbothioamide (**2**): Yield: 90%. M.p.: 213-215 °C. Anal. calcd. for $C_{14}H_{15}N_3OS$: C, 61.51; H, 5.53; N, 15.37. Found: C, 61.43; H, 5.46; N, 15.35%. FT-IR (KBr, ν, cm^{-1}): 3405 (OH), 3149 (N-NH), 1600 (C=N), 1537 ($C_{aro}O$), 1264 (C=S). ^1H NMR (500 MHz, DMSO-d_6, δ, ppm): 1.18 (t, 3H, CH_3), 3.62 (dd, 2H, CH_2), 7.22 (d, 1H, Ar-H), 7.39 (t, 1H, Ar-H), 7.57 (t, 1H, Ar-H), 7.85 (dd, 2H, Ar-H), 8.38 (bt, 1H, CS-NH), 8.46 (d, 1H, Ar-H), 9.06 (s, 1H, CH=N). ^{13}C NMR (125 MHz, DMSO-d_6, δ, ppm): 14.49 (CH_3), 30.62 (CH_2), 109.77-142.61 (C-aromatic), 156.30 (C=N), 177.42 (C=S); UV-Vis (DMSO, λ_{max}, nm): 320, 330, 370.

3. Results and discussion

3.1. Synthesis

The (*E*)-2-(3-ethoxy-2-hydroxybenzylidene)hydrazine carbothioamide (**1**) and (*E*)-*N*-ethyl-2-((2-hydroxynaphthalen-1-yl)methylene)hydrazinecarbothioamide (**2**) were prepared by the condensation reaction of 3-ethoxy-2-hydroxybenzaldehyde and thiosemicarbazide or 2-hydroxy-1-naphthaldehyde and 4-ethyl-3-thiosemicarbazide (Scheme 1). The compounds may exist in two tautomeric forms, either thione or thiol form (Scheme 2). The compounds are air stable and soluble in DMF, DMSO, and rare soluble in H_2O.

3.2. FT-IR analysis

The bands appeared at 3405 and 3149 cm^{-1} are attributed to the ν(OH) and ν(N-NH) for compound **2**, respectively. The imino group (C=N) for compound **2** gave a band at 1600-1609 cm^{-1}. The strong band observed at 1550 and 1537 cm^{-1} is attributed to ν(C_{aro} O) for compound **1** and **2**, respectively. The

thione group (C=S) for compound **1** and **2** gave a sharp stretching band at 1275 and 1264 cm^{-1}, respectively.

3.3. ^{1}H NMR analysis

The ^{1}H NMR spectra of compound **1** and **2** are shown in Figure 1 and 2, respectively. In compound **1**, the triplet signal at δ 1.37 ppm is attributed to CH_3 protons, the quartet signal at δ 4.04 ppm is attributed to CH_2 protons. The interaction between the aromatic protons produces triplet signal for C_5-H at δ 6.57 ppm, and doublet signals for C_4-H and C_6-H at δ 6.91 and 7.50 ppm, respectively. The singlet signals at δ 7.87 and 8.03 ppm are attributed to NH_2 protons. The OH proton show a broad signal at δ 9.13 ppm, whereas the observed singlet signals at δ 8.41 and 11.40 ppm are attributed to the CH=N and N-NH protons.

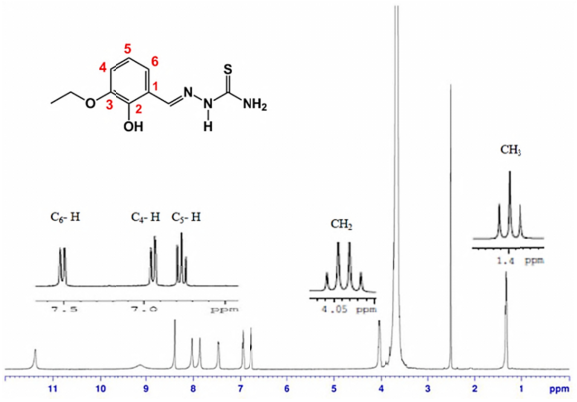

Figure 1. ^{1}H NMR spectrum of compound **1** in DMSO-d_6.

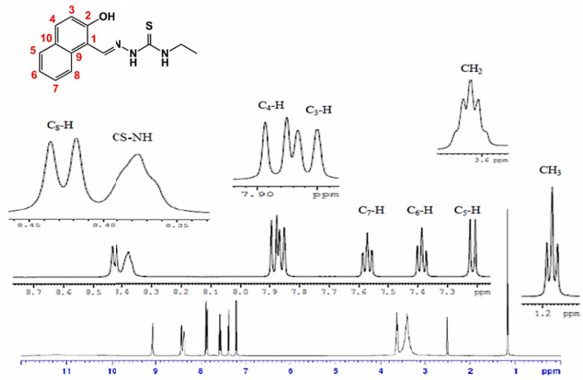

Figure 2. ^{1}H NMR spectrum of compound **2** in DMSO-d_6.

In compound **2**, the triplet signal at δ 1.18 ppm is attributed to CH_3 protons, the quintet signal at δ 3.62 ppm is attributed to CH_2 protons resulting from the interaction with CH_3 and NH protons. The interaction between the aromatic protons produces doublet signal at δ 7.22 ppm for C_5-H, triplet signals at δ 7.39 and 7.57 ppm for C_6-H and C_7-H, respectively, the interaction of C_3-H and C_4-H results a doublet of doublet signal at δ 7.85 ppm, whereas the C_8-H show a doublet signal at δ 8.46 ppm. The broad triplet signal that emerged at δ 8.38 ppm is attributed to CS-NH proton, the nuclear quadrupole interaction of ^{14}N (I = 1) causes to lower the lifetime of excited state of the protons which leads to broaden the resulting NMR signal. The CH=N proton appeared as a singlet signal at δ 9.06 ppm.

3.4. ^{13}C NMR analysis

Both the compounds **1** and **2** show the carbon signal of CH_3 at δ 14.50 ppm. The oxygen atom shifted the carbon signal of CH_2 to downfield more than nitrogen atom which shown at δ 64.15 and 30.62 ppm for compound **1** and **2**, respectively. The aromatic carbons of compound **1** appeared in the range from δ 114.06 to 146.17 ppm, whereas for compound **2** from δ 109.77 to 142.61 ppm. The signal at δ 177.51 ppm is attributed to the carbon of C=S and, the carbon signals of C=N are appeared at δ 146.95 ppm for compound **1**.

3.5. UV-Visible analysis

The electronic transition spectra of compound **1** and **2** shown in Figure 3, were measured in DMSO at room temperature. The compound **1** show two absorption bands at 295 and 312 nm which are attributed to the π → π* transition of aromatic ring and n → π* transition of the azomethine and thiolate function, respectively. The compound **2** show three absorption bands at 320 and 330 nm which are attributed to π → π* transition, and at 370 nm which attributed to n → π* transition.

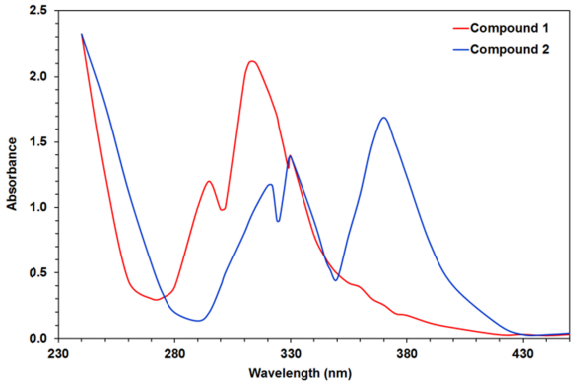

Figure 3. Electronic transitions of the compounds **1** and **2**.

3.6. Fluorescence analysis

The fluorescence emission spectra of compound **1** and **2** shown in Figure 4, were measured in DMSO at room temperature. The fluorescence emission is attributed to the π* → π transition rather than the π* → n transition because the quantum efficiency is greater and the lifetime is shorter than that for the π* → n transition [27]. The compounds **1** and **2** show a fluorescence emission bands at 378 nm. The compound **1** show second emission band at 520 nm may be due to formation of excimer molecule, which is arises when the rigidity and steric features succeed to bring the molecules close enough to limit that allows to energy transfer which leads to generate an excimer molecule [28].

3.7. X-ray crystallography diffraction analysis

The crystal data and refinement parameters for compounds **1** and **2** are summarized in Table 1. The bond lengths (Å), bond angles (°) and torsion angles (°) are given in Table 2, 3 and 4, respectively. The molecular structures are shown in Figure 5 and 6, respectively.

The compound **1** is a second monoclinic ($P2_1/c$) and is close to the molecule B of the previously reported ($P2_1$) form, which was isolated from an ethanol solution [29]. To a first approximation, the molecular structure found is similar, but three significant differences are noted.

Table 1. Crystal data and refinement parameters for compounds **1** and **2**.

Parameter	Compound 1	Compound 2
Chemical formula	$C_{10}H_{13}N_3O_2S$	$C_{14}H_{15}N_3OS$
Formula weight	239.30	273.36
Crystal system	Monoclinic	Monoclinic
Crystal description	Plate colorless	Needle yellow
Space group	$P2_1/c$	$P2_1$
a (Å)	12.8547(5)	9.2934(14)
b (Å)	5.9945(2)	5.0115(8)
c (Å)	16.0739(7)	14.736(2)
α (°)	90	90
β (°)	100.494(2)	103.620(3)
γ (°)	90	90
Volume (Å^3)	1217.90(8)	667.01(17)
Z	4	2
D_{calc} (g/cm^3)	1.305	1.361
Crystal size (mm)	0.07 × 0.11 × 0.49	0.03 × 0.09 × 0.50
Temperature (K)	100	100
Total data	16551	7884
Unique data	3589	3684
R_{int}	0.043	0.038
Observed data [I>2σ(I)]	2785	3196
R_1	0.0478	0.0401
wR_2	0.1025	0.0971
S	1.04	1.05

Table 2. Bond lengths for compound **1** and **2**.

Atom	Atom	Length, Å	Atom	Atom	Length, Å
Compound 1					
S1	C8	1.7017(16)	C1	C6	1.391(2)
O1	C1	1.3658(17)	C1	C2	1.409(2)
O2	C2	1.3675(18)	C2	C3	1.386(2)
O2	C9	1.4450(18)	C3	C4	1.405(2)
N1	C7	1.2845(19)	C4	C5	1.379(2)
N1	N2	1.3795(17)	C5	C6	1.408(2)
N2	C8	1.3470(19)	C6	C7	1.460(2)
N3	C8	1.327(2)	C9	C10	1.507(2)
Compound 2					
S1	C12	1.6856(19)	C3	C4	1.419(3)
O1	C1	1.355(2)	C4	C5	1.423(3)
N1	C11	1.296(2)	C4	C9	1.432(2)
N1	N2	1.379(2)	C5	C6	1.372(3)
N2	C12	1.357(2)	C6	C7	1.412(3)
N3	C12	1.339(2)	C7	C8	1.371(3)
N3	C13	1.464(3)	C8	C9	1.420(2)
C1	C10	1.403(2)	C9	C10	1.437(3)
C1	C2	1.411(3)	C10	C11	1.453(3)
C2	C3	1.368(3)	C13	C14	1.520(2)

Table 3. Bond angles for compound **1** and **2**.

Atom	Atom	Atom	Angle, °	Atom	Atom	Atom	Angle, °
Compound 1							
C2	O2	C9	117.59(12)	C5	C4	C3	120.98(14)
C7	N1	N2	115.06(13)	C4	C5	C6	120.29(14)
C8	N2	N1	120.20(13)	C1	C6	C5	118.82(13)
O1	C1	C6	119.52(13)	C1	C6	C7	119.27(13)
O1	C1	C2	119.69(13)	C5	C6	C7	121.89(13)
C6	C1	C2	120.78(13)	N1	C7	C6	120.92(13)
O2	C2	C3	126.39(14)	N3	C8	N2	117.09(14)
O2	C2	C1	113.67(13)	N3	C8	S1	123.86(12)
C3	C2	C1	119.93(14)	N2	C8	S1	119.05(11)
C2	C3	C4	119.19(14)	O2	C9	C10	107.23(14)
Compound 2							
C11	N1	N2	115.99(14)	C8	C7	C6	121.40(17)
C12	N2	N1	120.78(15)	C7	C8	C9	121.31(17)
C12	N3	C13	124.43(17)	C8	C9	C4	117.53(17)
O1	C1	C10	122.55(17)	C8	C9	C10	123.23(16)
O1	C1	C2	115.94(16)	C4	C9	C10	119.23(15)
C10	C1	C2	121.50(17)	C1	C10	C9	118.75(16)
C3	C2	C1	119.91(16)	C1	C10	C11	120.58(17)
C2	C3	C4	121.37(18)	C9	C10	C11	120.64(15)
C3	C4	C5	121.33(17)	N1	C11	C10	122.02(16)
C3	C4	C9	119.23(17)	N3	C12	N2	116.47(16)
C5	C4	C9	119.44(16)	N3	C12	S1	123.33(15)
C6	C5	C4	121.48(19)	N2	C12	S1	120.20(13)
C5	C6	C7	118.83(19)	N3	C13	C14	108.89(18)

The compound **1** which was isolated from the DMF solution show the *syn* configurations of O1 atom with respect to O2 atom (torsion angle: O1-C1-C2-O2 = 0.16(19)°) and C2 atom with respect to C5 atom (torsion angle: C1-C2-C3-C5 = 0.6(2)°), whereas in the reported $P2_1$ form, the corresponding atoms of molecule B show the *anti* configurations of O3 atom with respect to O4 (torsion angle: O3-C11-C12-O4 = -1.1(7)°) and C12 atom with respect to C15 (torsion angle: C12-C13-C14-C15 = -0.8(8)°).

Table 4. Torsion angles for compound **1** and **2**.

A	B	C	D	Angle, °	A	B	C	D	Angle, °
Compound 1									
C7	N1	N2	C8	176.36(14)	C2	C1	C6	C5	-0.1(2)
C9	O2	C2	C3	-7.0(2)	O1	C1	C6	C7	-1.0(2)
C9	O2	C2	C1	172.11(13)	C2	C1	C6	C7	178.34(13)
O1	C1	C2	O2	0.15(19)	C4	C5	C6	C1	0.5(2)
C6	C1	C2	O2	-179.14(13)	C4	C5	C6	C7	-177.96(14)
O1	C1	C2	C3	179.34(13)	N2	N1	C7	C6	177.22(13)
C6	C1	C2	C3	0.1(2)	C1	C6	C7	N1	-174.45(14)
O2	C2	C3	C4	178.79(14)	C5	C6	C7	N1	4.0(2)
C1	C2	C3	C4	-0.3(2)	N1	N2	C8	N3	-3.3(2)
C2	C3	C4	C5	0.6(2)	N1	N2	C8	S1	176.26(11)
C3	C4	C5	C6	-0.7(2)	C2	O2	C9	C10	-172.87(14)
O1	C1	C6	C5	-179.43(13)					
Compound 2									
C11	N1	N2	C12	-177.57(17)	O1	C1	C10	C9	178.91(17)
O1	C1	C2	C3	-178.89(17)	C2	C1	C10	C9	-0.9(3)
C10	C1	C2	C3	0.9(3)	O1	C1	C10	C11	-2.6(3)
C1	C2	C3	C4	-0.4(3)	C2	C1	C10	C11	177.62(17)
C2	C3	C4	C5	179.26(18)	C8	C9	C10	C1	-178.85(18)
C2	C3	C4	C9	0.0(3)	C4	C9	C10	C1	0.4(2)
C3	C4	C5	C6	-179.95(19)	C8	C9	C10	C11	2.7(3)
C9	C4	C5	C6	-0.7(3)	C4	C9	C10	C11	-178.10(16)
C4	C5	C6	C7	0.8(3)	N2	N1	C11	C10	-179.77(16)
C5	C6	C7	C8	-0.4(3)	C1	C10	C11	N1	-0.2(3)
C6	C7	C8	C9	-0.3(3)	C9	C10	C11	N1	178.28(17)
C7	C8	C9	C4	0.4(3)	C13	N3	C12	N2	-179.84(17)
C7	C8	C9	C10	179.66(18)	C13	N3	C12	S1	0.1(3)
C3	C4	C9	C8	179.33(18)	N1	N2	C12	N3	-3.3(3)
C5	C4	C9	C8	0.0(2)	N1	N2	C12	S1	176.81(14)
C3	C4	C9	C10	0.1(2)	C12	N3	C13	C14	-176.24(19)
C5	C4	C9	C10	-179.24(17)					

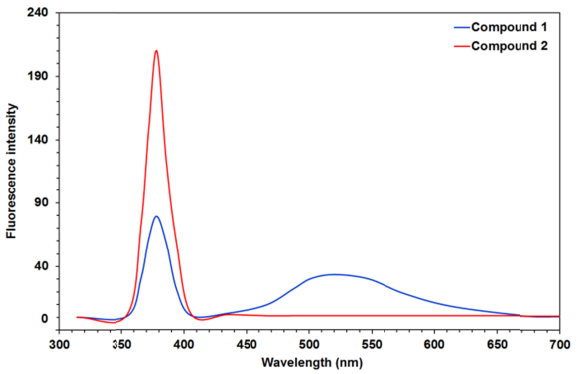

Figure 4. Fluorescence emission spectra of the compounds **1** and **2**.

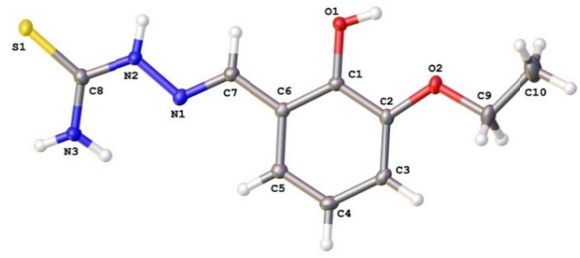

Figure 5. Molecular structure of compound **1**.

In addition, the compound **1** show the *anti* configuration of C3 atom with respect to C6 atom (torsion angle: C3-C4-C5-C6 = -0.7(2)°), whereas the corresponding atoms of molecule B show the *syn* configuration (torsion angle: C13-C14-C15-C16 = 1.2(8)°). Moreover, the value of β angle in the $P2_1/c$ form is 100.494(2)°, whereas that for the reported $P2_1$ is close to 90° and equal to 90.238(3)°. A significant difference arises from the calculated refinement parameters of R_1, wR_2 and S, which are 0.0478, 0.1025 and 1.04; and 0.056, 0.119 and 0.92, for $P2_1/c$ and $P2_1$, respectively. Furthermore, the compound **1** in $P2_1/c$ form is centrosymmetric, whereas the $P2_1$ form is non-centrosymmetric [30].

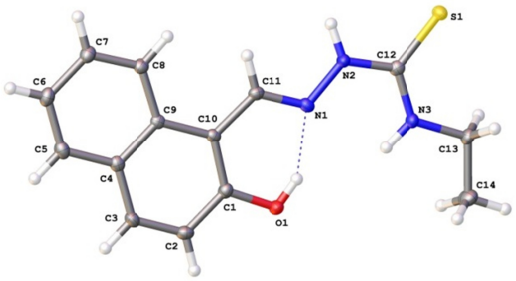

Figure 6. Molecular structure of compound **2**.

The prepared compounds show different structures based on the geometry of N1 atom in relation to C1 atom and C5 or C9 atom. In compound **1**, the N1 atom shows the *trans* geometry in relation to C1 atom and the *cis* geometry in relation to C5 atom. These geometries prevent the formation of intrahydrogen bonding of O1-H···N1. Whereas, in compound **2**, the N1 show the *cis* geometry in relation to C1 atom and the *trans* geometry in relation to the corresponding of C9 atom. These geometries allow the formation of intrahydrogen bonding of O1-H···N1. Both the compounds the N1 atom shows the *cis* geometry in relation to N3 atom and the *trans* geometry in relation to S1 atom. The bond distances of S1-C and C-N2 are 1.7015(18) and 1.347(2) Å and, 1.6854(19) and 1.357(3) Å, respectively. These distances confirmed that the compounds exist in thione form in sold state, which are changes upon complexation to thiol form [31].

Moreover, the compound **1** in monoclinic $P2_1/c$ crystal system with the presence of inversion center is centro-symmetric as shown in Figure 7, and show three planes. The first plane includes N1-N3, C8 and S1, the second plane includes O1, C1, C2 and C5-C7 and the third plane includes C3, C4, O2, C9 and C10. The dihedral angles between the first and second planes is 176.36(14)°, and between the second and third planes is 172.11(13)°. By contrast, the compound **2** in

monoclinic $P2_1$ crystal system with the absence of inversion center is non-centrosymmetric as shown in Figure 8, and show two planes. The first plane includes the aromatic rings and C11, and the second plane includes N1-N3, O1, S1 and C12-C14. The dihedral angle between the two planes is -179.77 (17)°.

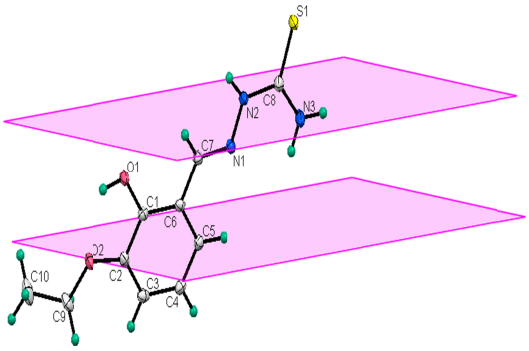

Figure 7. Crystal structure planes of compound **1**.

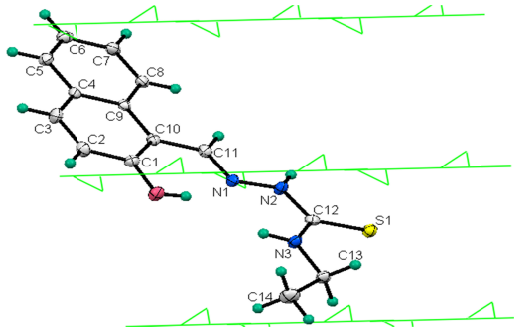

Figure 8. Crystal structure planes of compound **2**.

The crystal structure of compound **1** molecules form centrosymmetrically related dimmers through the intermolecular hydrogen bonds N2–H1···O1 and O1–H1···S1 (symmetry code: -*x*, -*y*, -*z*), and N3–H···S1 (symmetry code: 1-*x*, -*y*, -*z*). These hydrogen bonds are stabilizing the packing of the compound **1** molecule in crystal lattice (Figure 9). By contrast, the crystal structure of compound **2** molecules form centrosymmetrically related dimmers through the intermolecular hydrogen bonds N2–H1···S1 and C11–H11A···S1 (symmetry code: 1-*x*, -1/2+*y*, 1-*z*), and C2–H2A···O1 (symmetry code: 1-*x*, -1/2+*y*, 2-*z*). These hydrogen bonds allow the compound **2** molecules to be stacked along the *b*-axis via π-π interactions which are stabilize the packing crystal structure of the compound. Moreover, the orientation of the phenyl rings (torsion angle C1–C10–C11–N1 = - 0.2(3)°) is stabilized by O1–H1···N1 hydrogen bond, and the *syn* conformation of the C13 atom in respect to S1 atom (torsion angle C13–N3–C12–S1 = 0.1(3)°) is stabilized by N3–H1···N1 hydrogen bond (Figure 10).

3.8. DNA cleavage activity

The agarose gel electrophoresis patterns of the compounds **1** and **2** are shown in Figure 11. From lane 1 to 8, the compound **1** show the naturally fast migration form which is related to the closed circular supercoiled form (SC, form I). At concentration 4.5 μM (lane 9) and 5.0 μM (lane 10), the compound show the slow migration form which is related to the open circular relaxed form (OC, form II) [32]. Whereas, the compound **2** show higher cleavage activity, it can nick one of the DNA strands to produce the OC form at concentration 1 μM (lane 4). The presence of terminal *N(4)*-ethyl and  groups are increase the lipophilic properties of compound **2** which are increase the affinity with the hydrophobic medium of DNA together with the geometrical and conformational structures that may be lead to an intimate association with DNA, which in turn increases the action of compound to cleave DNA. The compounds show different action regarding the SC form. In compound **1**, the size of SC fragments increases with increase the concentration of the compound, whereas for compound **2** the size of SC fragments decreases with increase the concentration of the compound. Furthermore, the addition of 6 μM of both compounds (lane 11) to DNA leads to a rigid product which may refers to denaturation of DNA.

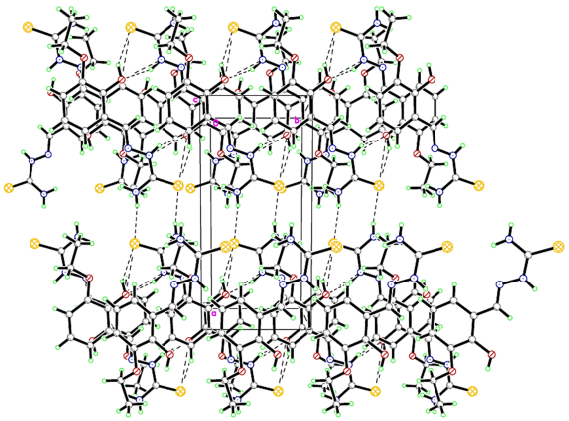

Figure 9. Crystal packing structure of compound **1**, viewed along *c* axis. Hydrogen bonds are shown as dashed lines.

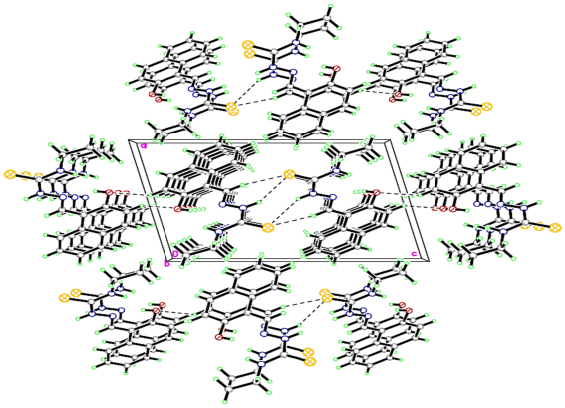

Figure 10. Crystal packing structure of compound **2**, viewed along *b* axis. Hydrogen bonds are shown as dashed lines.

The DNA cleavage study was investigated in the presence of fixed amount (4.5 μM) of H_2O_2. The cleavage action can not take place in presence of the compound alone (lane 2) or H_2O_2 alone (lane 3). Furthermore, the DNA cleavage was investigated in the presence of the hydroxyl radical scavenger DMSO. If the cleavage action depends on the hydroxyl radical, the DMSO leads to inhibit the nuclease activity of the compounds. These observations confirm that cleavage action depends on the concentration of the compounds **1** and **2** but in presence of H_2O_2. Our suggestion that the compounds exist in anion form (Scheme 2) in presence of H_2O_2, and the compound anion involves a nucleophilic attack at the phosphate backbone of DNA, which subsequent leads to cleave the DNA strand.

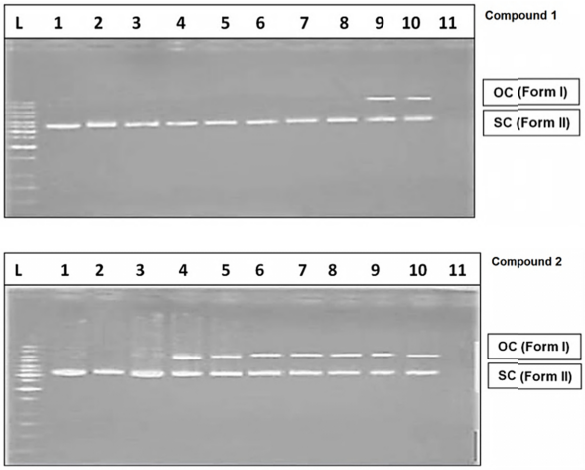

Figure 11. Agarose gel electrophoresis patterns of pBR 322 for the compounds **1** and **2**.

4. Conclusions

Different analytical and spectral methods were used for the characterization of two new thiosemicarbazones derivatives. The X-ray diffraction analysis shows that the compounds possess different geometrical and conformational structures. The nuclease activity of the compounds against pBR 322 circular plasmid DNA was investigated using agarose gel electrophoresis assay. The compound **2** showed higher nuclease activity than compound **1**.

Supplementary material

CCDC 953517 and 958081 contain the supplementary data for compound **1** and **2**, respectively. These data can be obtained free of charge at http://www.ccdc.cam.ac.uk/data_request/cif.

References

[1]. Leigh, M.; Castillo, C. E.; Raines, D. J.; Duhme-Klair, A. K. *Chem. Med. Chem.* **2011**, *6*, 612-616.
[2]. Hussein, M. A.; Guan, T. S.; Haque, R. A.; Ahamed, M. B. K.; Majid, A. M. S. A. *Polyhedron* **2015**, *85*, 93-103.
[3]. Ali, A. Q.; Teoh, S. G.; Eltayeb, N. E.; Ahamed, M. B. K.; Majid, A. M. S. A. *Polyhedron* **2014**, *74*, 6-15.
[4]. Ngan, N. K.; Lo, K. M.; Wong, C. S. R. *Polyhedron* **2012**, *33*, 235-251.
[5]. Hussein, M. A.; Iqbal, M. A.; Asif, M.; Haque, R. A.; Ahamed, M. B. K.; Majid, A. M. S. A.; Guan, T. A. *Phosphorus, Sulfur Silicon Relat. Elem.* **2015**, *190*, 1498-1508.
[6]. Argueelles, M. C. R.; Touceda, P. T.; Cao, R.; Deibe, A. M. G.; Pelagatti, P.; Pelizzi, C.; Zani, F. *J. Inorg. Biochem.* **2009**, *103*, 35-42.
[7]. Ferrari, M. B.; Bisceglie, F.; Pelosi, G.; Tarasconi, P.; Albertini, R.; Pinelli, S. *J. Inorg. Biochem.* **2001**, *87*, 137-147.
[8]. Kowol, C. R.; Berger, R.; Eichinger, R.; Roller, A.; Jakupec, M. A.; Schmidt, P. P.; Arion, V. B. Keppler, B. K. *J. Med. Chem.* **2007**, *50*, 1254-1265.
[9]. Osman, H.; Arshad, A.; Lam, C. K.; Bagley M. C. *Chem. Cent. J.* **2012**, *6*, 32-42.
[10]. Mendes, I. C.; Soares, M. A.; Dos Santos, R. G.; Pinheiro, C.; Beraldo, H. *Eur. J. Med. Chem.* **2009**, *44*, 1870-1877.
[11]. Bernhardt, P. V.; Sharpe, P. C.; Islam, M.; Lovejoy, D. B.; Kalinowski, D. S.; Richardson, D. R. *J. Med. Chem.* **2009**, *52*, 407-415.
[12]. Baldini, M.; Ferrari, M. B.; Bisceglie, F.; Pelosi, G.; Pinelli, S. *Inorg. Chem.* **2003**, *42*, 2049-2055.
[13]. Bisceglie, F.; Baldini, M.; Belicchi-Ferrari, M.; Buluggiu, E.; Careri, M.; Pelosi, G.; Pinelli, S.; Tarasconi, P. *Eur. J. Med. Chem.* **2007**, *42*, 627-634.
[14]. Baodui, W.; Zhengyin, Y.; Minghua, L.; Jun, H.; Qin, W.; Zhongnig, C. *J. Organomet. Chem.* **2009**, *694*, 4069-4075.
[15]. Lobana, T. S.; Sharma, R.; Bava, G.; Khanna, S. *Coord. Chem. Rev.* **2009**, *253*, 977-1055.
[16]. Anderson, B. J.; Shalit, Z. A.; Jasinski, J. P. *Acta Cryst. E* **2014**, *70*, o732-o732.
[17]. Casas, J. S.; Garcia, T. M. S.; Sordo, J. *Coord. Chem. Rev.* **2000**, *209*, 197-261.
[18]. Beraldo, H.; Gambino, D. *Mini-Rev. Med. Chem.* **2004**, *4*, 31-39.
[19]. Dilovic, I.; Rubcic, M.; Vrdoljak, V.; Pavelic, S. K.; Kralj, M.; Piantanida, I.; Cindric, M. *Bioorg. Med. Chem.* **2008**, *16*, 5189-5198.
[20]. Hussein, M. A.; Guan, T. S.; Haque, R. A.; Ahamed, M. B. K.; Majid, A. M. S. A. *J. Coord. Chem.* **2014**, *67*, 714-727.
[21]. Gomez-Saiz, P.; Gil-Garcia, R.; Maestro, M. A.; Pizarro, J. L.; Arriortua, M. I.; Lezama, L.; Rojo, T.; Gonzalez-Alvarez, M.; Borras, J.; Garcia-Tojal, J. *Inorg. Biochem.* **2008**, *102*, 1910-1920.
[22]. Lu, J.; Guo, H.; Zeng, X.; Zhang, Y.; Zhao, P.; Jiang, J.; Zang, L. *Inorg. Biochem.* **2012**, *112*, 39-48.
[23]. Aguirre, Y. C.; Borras, J.; Castineiras, A.; Garcia-Monteagudo, J. M.; Garcia- Santos, I.; Niclos, J.; West, D. X. *Eur. J. Inorg. Chem.* **2006**, *2006*, 1231-1244.
[24]. Lobana, T. S.; Kumari, P.; Butcher, R. J. *Inorg. Chem. Commun.* **2008**, *11*, 11-14.
[25]. Lhuachan, S.; Siripaisarnpipat, S.; Chaichit, N. *Eur. J. Inorg. Chem.* **2003**, *2003*, 263- 267.
[26]. Sheldrick, G. M. *Acta Cryst.* **2008**, *A64*, 112-122.
[27]. Yeung A. S.; Frank, C. W.; Singer, R. E. *Polymer* **1990**, *31*, 1092-1099.
[28]. Bains, G. K.; Kim, S. H.; Sorin, E. J.; Narayanaswami, V. *Biochemistry* **2012**, *51*, 6207- 6219.
[29]. Ardakani, A. A.; Kargar, H.; Kia, R.; Tahir, M. N. *Acta Cryst. E* **2012**, *68*, o340-o341.
[30]. Ok, M. K.; Chi, E. O.; Halasyamani, S. *Chem. Soc. Rev.* **2006**, *35*, 710-717.
[31]. Hussein, M. A.; Guan, T. S.; Haque, R. A.; Ahamed, M. B. K.; Majid, A. M. S. A. *Spectrochim. Acta A* **2015**, *136*, 1355-1348.
[32]. Gao, E. J.; Zhu, M. C.; Huang, Y.; Liu, L.; Ma, S.; Shi, C. Y. *Eur. J. Med. Chem.* **2010**, *45*, 1034-1041.